Fracture Behavior of Glass Bead Filled Epoxies: Cleaning Process of Glass Beads

JONGHWI LEE,[1,*] ALBERT F. YEE[1,2]

[1] Macromolecular Science and Engineering Center, University of Michigan, Ann Arbor, Michigan 48109

[2] Department of Materials Science and Engineering, University of Michigan, Ann Arbor, Michigan 48109

Received 2 December 1999; accepted 14 January 2000

ABSTRACT: Inorganic particles are commonly cleaned with solvents such as alcohols before being incorporated into thermoset polymers as fillers or tougheners, but the role of the cleaning process has never been examined. In this study, the effect of the cleaning process on the fracture behavior of particulate composites is investigated using glass bead filled epoxies as model systems. The cleaning process is shown to be a simple method to strengthen the interface between the glass beads and the epoxy matrix. Although the chemistry of the glass bead surface is unlikely to be altered by the cleaning process, submicron particles that exist on the glass bead surfaces are removed by cleaning with distilled water or ultrasonic vibration. The removal of submicron particles increases the interfacial strength between the glass beads and the matrix and changes the tensile strength of the composites. However, the modulus and fracture toughness of the composites is not significantly dependent on the cleaning process. Thus, it may be the case that debonding of the glass beads is not one of the major energy dissipating mechanisms in the fracture of glass bead filled thermoset systems. © 2000 John Wiley & Sons, Inc. J Appl Polym Sci 79: 1371–1383, 2001

Key words: fracture; toughness; epoxies; filler; surface

INTRODUCTION

Inorganic particles have been widely used as fillers in thermoset polymers for various purposes. The use of these particles not only reduces the cost of thermoset polymer products but also changes other properties such as the modulus, hardness, strength, thermal properties, rheological properties, and fracture toughness.[1–4] Among these changes, the modification of the fracture toughness is both important and interesting. From the previous studies using the fundamental fracture mechanics approach,[5] inorganic particles have been found to be effective tougheners for thermoset polymers, although inorganic particle inclusion does not increase the fracture toughness of composites as dramatically as rubber particle inclusion.[3,4] This means that for the same volume fraction of toughener, rubber particles produce a much more significant toughening effect than inorganic particles.

Despite the less dramatic toughening effect, inorganic particle toughening has an advantage over rubber toughening: although rubber particles in polymer matrices usually cause the modulus and the hardness of toughened polymers to fall below those of the neat (unmodified) matrix,

Correspondence to: A. F. Yee (afyee@engin.umich.edu).

* *Present address:* Department of Chemical Engineering and Materials Science, University of Minnesota, Minneapolis, MN 55455.

Contract grant sponsor: Specialized Materials Science Research Center (NIH); contract grant number: DEO 9296-09.

Journal of Applied Polymer Science, Vol. 79, 1371–1383 (2001)

the use of inorganic particles can increase modulus, hardness, *and* fracture toughness.[3,6] This desirable enhancement of the mechanical properties makes inorganic particle toughening useful in various applications, including electronic packaging, dental restorative materials, fiber composites, and so forth.

Cleaning inorganic particles with alcohols is frequently performed to remove any surface contamination in the experiments on inorganic particle filled composites.[7,8] However, no study on the effect that these cleaning processes have on mechanical properties has yet been performed. Furthermore, in most of the previous reports[7,8] no specific reasons for the selection of cleaning agents are given. Thus, as far as we know, the actual roles of cleaning agents still remain unexamined. It can be expected that cleaning agents alter the interfacial strength between the particles and the matrix.

This article reports the first study on the action of cleaning processes on the fracture toughness of composites. As models for inorganic particle toughened thermosets, glass bead filled diglycidyl ether of bisphenol A (DGEBA)/4,4′-diaminodiphenylsulfone (DDS) epoxies were used. Distilled water and isopropanol were chosen as cleaning agents, and the resulting composites were compared with composites prepared by using glass beads as received. This study on cleaning processes adds to the cumulative finding[6] that the interfacial strength between glass beads and the matrix is not an important factor in determining the fracture toughness of particulate composites. This study is also one of the initial steps to discovering new general underlying mechanisms of inorganic particle toughening.[10]

EXPERIMENTAL

Materials

A solid DGEBA epoxide resin, DER 661® (molecular weight = 1750–1950), was provided by the Dow Chemical Co. Spheriglass® A glass beads (soda-lime glass) with no surface treatment were obtained from Potters Industry Co. An amine curing agent, DDS (98%), other solvents, and reagents were obtained from Aldrich Chemical Co. They were used without any further purification.

Cleaning of the glass beads was performed as follows: the glass beads were dispersed in a solvent (distilled water or isopropanol, glass beads/solvent = 0.29 g/mL) under mechanical stirring at room temperature for 6 h, and then the solvent was removed. This cleaning procedure was repeated 3 times, followed by drying of the cleaned glass beads under a vacuum at 70°C for 12 h. Before being incorporated into the epoxy resins the cleaned glass beads were screened by using a 75-μm sieve (mesh size = 200) to remove large aggregates.

Preparation of Composites

The DER® 661 was first melted at 160°C and degassed under a vacuum for about 1.5 h. It was then mixed with glass beads for 1.5 h and with stoichiometric amounts of DDS for 40 min. This degassed mixture was poured into a preheated metal mold and vertically mounted in a convection oven, where it was cured for 16 h at 160°C followed by 2 h at 200°C. After this, the cured resin was allowed to cool slowly to room temperature in the oven. The viscosity of the epoxide was high enough to prevent the glass beads from settling to the bottom of the mold during curing. The amount of glass beads in the epoxy resins was changed from 0 to 30 vol %.

Characterization

The liquid-phase sedimentation method was used to measure the average diameters of the glass beads with a Horiba CAPA-700 particle size distribution analyzer, which is a noncontact measuring method. Particle size data were obtained from the change in particle concentrations on the basis of light transmission. Glass beads (0.01 wt %) and sodium hexametaphosphate (dispersion agent, 0.1 wt %) were dispersed in ethylene glycol (medium) and used for the measurement. At least three repeated measurements were used to give the average diameters in Table I and the typical distribution curves in Figure 1. To verify these data, direct measurements were performed using a Nikon Microphot II optical microscope (OM) and a Sony DXC-151A color video CCD camera (resolution = 768 × 493 pixels). The average diameters from more than 150 measurements using the OM are given in Table I. Although the magnification limit of the OM makes it difficult to measure particles of 1 μm or less, a reasonable agreement between the liquid-phase sedimentation and the optical microscopy results was found. The basic physical properties of the ep-

Table I Designation of Glass Beads Used in Experiment

Designation	Mean Diameter[a] (μm)	Mean Diameter[b] (μm)	Treatment
u-LG	2.6		As received
SG	3.3	4.1	Cleaned with distilled water
u-LG	25.2		As received
LG	24.4	27.9	Cleaned with distilled water

[a] The mean diameter obtained using a particle size analyzer.
[b] The mean diameter obtained using an optical microscope.

oxy matrix (designation: 661) and the glass beads are given in Table II.

Fracture Toughness Assessment and Microscopy

The critical stress intensity factor (K_{IC}) was measured by fracturing single edge notched (SEN) type specimens in the 3-point bend (3PB) geometry. Glass bead filled epoxies were first cut into the geometry (6.35 mm specimen thickness, B, and 12.7 mm width, W) that meets the plane-strain condition requirement (ASTM E399), $B > 2.5(K_{IC}/\sigma_y)^2$ (e.g., $B > 2.1$ mm for 30 vol % LG/661). The surfaces of the specimens were then polished with silicon carbide (SiC) grinding disks (80, 250, 400, 600, and 1000 grit size). A sharp notch in the SEN-3PB specimens was prepared by tapping with a mallet a razor blade inserted into specimens. Before the insertion, the razor blades were immersed in liquid nitrogen until boiling around it stopped. To avoid any artifacts from the razor blades, the sizes of all resulting initial cracks were confirmed to be longer than the insertion length of the razor blades. This meant that the cracks had been wedged open. A screw-driven Instron machine (Instron 4502) was used to fracture 12–18 samples for one composite material (2.54 mm/min crosshead speed, 50.8 mm span). The K_{IC} values were calculated using the relationship[12,13]

$$K_{IC} = Y \frac{3PS\sqrt{a}}{2BW^2}$$

$$Y = 1.93 - 3.07(a/W) + 14.53(a/W)^2 - 25.11(a/W)^3 + 25.80(a/W)^4 \quad (1)$$

where Y is a shape factor, P is the load at failure, S is the length of the span, and a is the crack length. Critical strain energy release rates (G_{IC}) were calculated from K_{IC} values using the following relationship[13] without correcting for plane-strain conditions:

$$G_{IC} = \frac{K_{IC}^2}{E} \quad (2)$$

where E is the Young's modulus of the composites. The true G_{IC} values of our systems that meet plane-strain conditions can be obtained by multiplying the right term of eq. (2) by $(1 - \nu^2)$, where ν is Poisson's ratio.[13] Nonetheless, eq. (2) was used in this study because the precise values of Poisson's ratio were not measured, although they

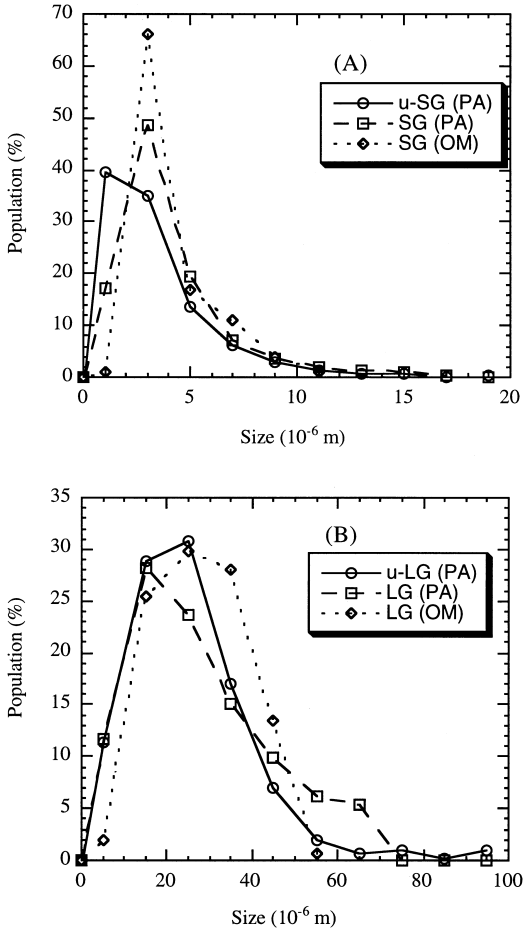

Figure 1 Particle size distribution curves for the (A) small glass beads (SG) or (B) large glass beads (LG) used in this experiment. The data were obtained by using a particle size analyzer (PA) or an optical microscope (OM).

Table II Physical and Mechanical Properties of Epoxy Matrix Materials and Glass Beads

Materials	Density (g/mL)	T_g (°C)	Modulus (GPa)	Yield Stress (MPa)	Solubility Parameter[45]
661 (DER® 661/DDS)	1.204	124	2.8	88	11.5–13[a]
Glass beads (Spheriglass® A glass beads)	2.5	Softening point = 704	70		

are expected to be quite similar; thus, correcting for the plane-strain condition cannot change the major results obtained from the G_{IC} analyses.

Small tensile specimens ($15 \times 5 \times 7$ mm gauge section) were used in the uniaxial tensile tests. The surface of the specimens was polished using SiC grinding disks (80, 240, 400, and 600 grit size) to remove surface defects. At least five specimens were tested for each composition, and the crosshead speed was 2.54 mm/min.

A scanning electron microscope (SEM, Hitachi S-800) was used to observe the fracture surface of SEN-3PB specimens coated with a thin layer of gold–palladium to reduce charge buildup. The accelerating voltage was either 5 or 3 kV.

RESULTS AND DISCUSSION

Characterization of Glass Beads

To check possible surface contamination of the as-received glass beads by organic compounds, X-ray photoelectron spectroscopy (XPS), NMR spectrometry, CHN analysis, and mass spectrometry were used. XPS results were obtained using a Perkin–Elmer PHI 5400 X-ray photoelectron spectroscope with an Al X-ray source. The results showed a significant amount of carbon species present on the surface of the glass beads. However, these results cannot be used as evidence for the existence of any organic materials that can effectively change the interfacial strength between the glass beads and epoxy matrix, because the surface of the glass beads is normally covered with an adsorbed carbonaceous overlayer.[14] Another trial to detect the existence of possible organic compounds on the surface of the glass beads was by NMR. After dispersing glass beads in a solvent (H_2O or toluene) under mechanical stirring for more than 6 h, the filtered solvent was completely dried in an NMR specimen tube that was analyzed in FT-NMR analysis. No organic compound was detected in any of the analyses on the tube. Furthermore, nothing was detected in the CHN analysis and mass spectrometry on the concentrated filtered solvent. Thus, it was believed that the as-received glass beads were free of organic compounds as the manufacturer claimed, so any cleaning procedure for the purpose of removing organic compounds did not seem necessary.

Figure 1 shows the typical particle size distributions of glass beads. Generally, the distribution data obtained by the direct OM observation gave reasonable agreements with those obtained by the liquid sedimentation method. In Figure 1(A) the slight difference among the distribution curves at around the 1-μm size region may be worth mentioning. Although the difference is very small, the as-received glass beads do possess a slightly higher amount of small (<2 μm) particles than cleaned glass beads. This is consistent with the finding that froth formed on the surface of the water during the cleaning process. The OM examination of the dried froth showed that there were submicron particles. Because they were removed during the cleaning process, cleaned glass beads must have less of these submicron particles. The following discussion on SEM micrographs again shows the premise that the cleaning process can remove submicron particles.

Because previous solubility and leaching resistance studies on glasses[15] and our surface contamination study described above generally indicate that the surface chemistry of glasses is hardly changed under the mild conditions of the cleaning procedure, it is more useful to focus on the topographical changes of the surface that are due to the cleaning process. Figure 2 shows the surface of glass beads treated by the four different kinds of methods. Many submicron particles, which can act as defects in resulting composite materials, adhere to the surface of the as-received glass beads [Fig. 2(A)] and those cleaned with isopropanol [Fig. 2(B)] by mainly electrostatic force. However, the surfaces of the other two glass

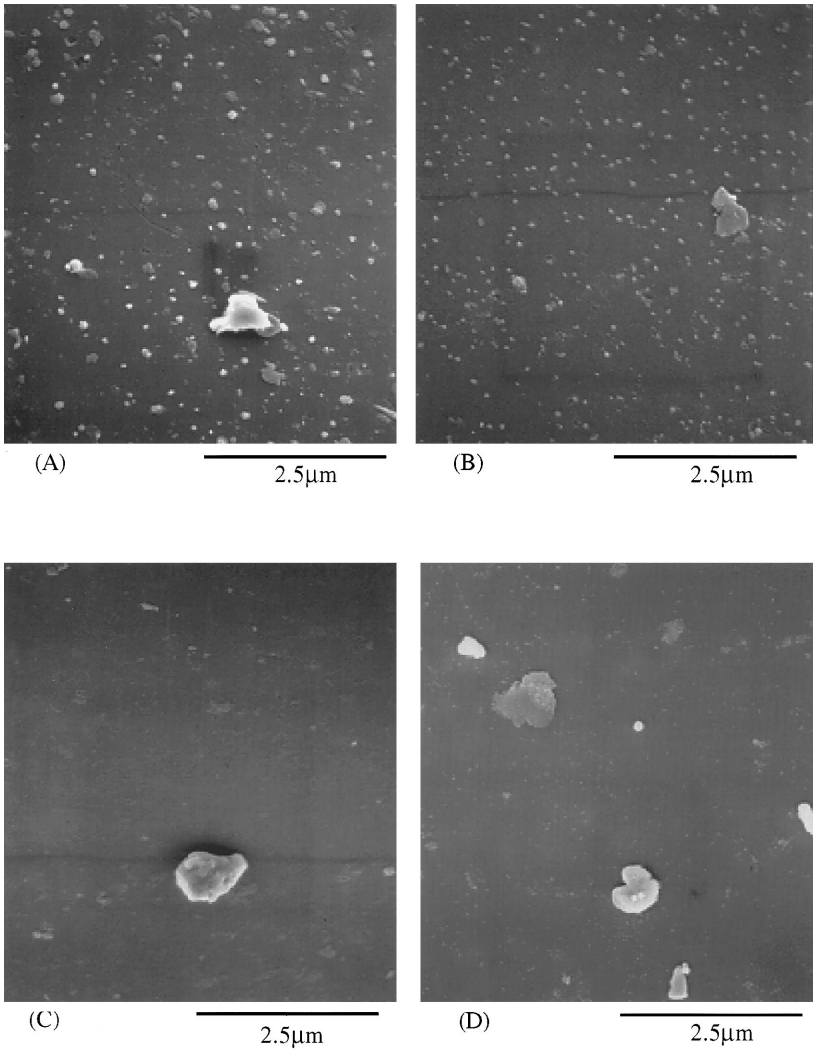

Figure 2 SEM micrographs of the surface of the glass beads (LG) (A) as received, (B) cleaned with isopropanol, (C) cleaned with distilled water, and (D) cleaned with isopropanol in an ultrasonic bath.

beads [Fig. 2(C,D)] do not have a significant amount of these particles. Although isopropanol cannot remove submicron particles from the surface of glass beads, Figure 2(C) reveals that distilled water can remove these particles during the cleaning process. In fact, it is reasonable that water is more powerful in removing these particles than isopropanol. This might be mainly because the surface energy of water (72.8 dyne/cm^2 at 20°C) is closer to that of glass (≈100–500 dyne/cm^2) than that of isopropanol (23.8 dyne/cm^2 at 20°C).[15–17]

Nevertheless, even in isopropanol, submicron particles can be removed by ultrasonic vibration as can be seen in Figure 2(D). In this cleaning process, as-received glass beads were dispersed for 6 h in isopropanol under ultrasonic vibration using a Cole–Parmer 8851 Ultrasonic Bath (50/60 Hz, 115 V, 1.5 A). After the isopropanol was filtered out, the glass beads were dried and used for the preparation of the composite like the other cleaning processes.

Mechanical Properties of Composites

Figure 3 shows the K_{IC} of glass bead filled epoxies. The error bar is the standard deviation for more than 12 measured values. The most distinct thing in this figure is that the cleaning process does not seem to be an important factor in determining the fracture toughness of composites. The G_{IC} calculated from the K_{IC} and modulus data can

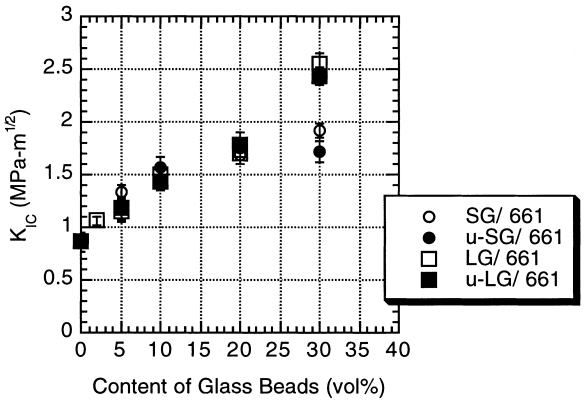

Figure 3 The critical stress intensity factor versus the glass bead content for glass bead filled epoxies.

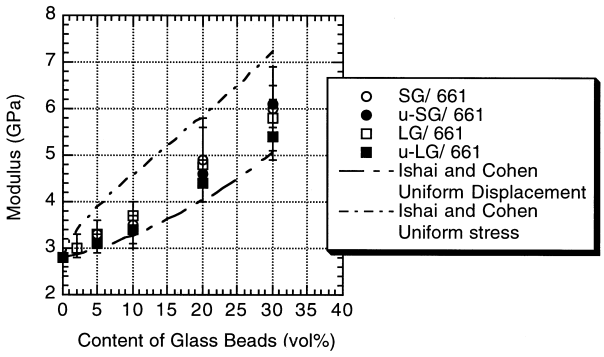

Figure 5 The tensile modulus versus the glass bead content for glass bead filled epoxies.

be found in Figure 4. The general trend of this figure is the same as that of Figure 3: the cleaning process does not make any significant difference in the fracture toughness of the composites.

Figure 5 shows the moduli of the composites prepared in the present experiment in which the range between the maximum and minimum values obtained from five different measurements for a composition is shown as an error bar. Again, the cleaning process was found to not be a factor in determining the modulus of the composites. In the microscopy studies discussed later, the cleaning process was found to be useful for improving the interfacial strength between glass beads and the epoxy matrix. However, the tensile modulus of the composites did not reflect this improvement, although it was expected to increase because of more effective load transfer across the interface that was due to improved interfacial strength. In fact, this result was not very surprising because it was reported[7,17–22] that the common surface treatments of glass beads to improve the interfacial strength, such as silation, cannot significantly increase the modulus of composites. Modulus is a material property obtained at very small strains. Under this condition, the relatively small difference in the interfacial strength due to surface treatments may be scarcely noticeable.

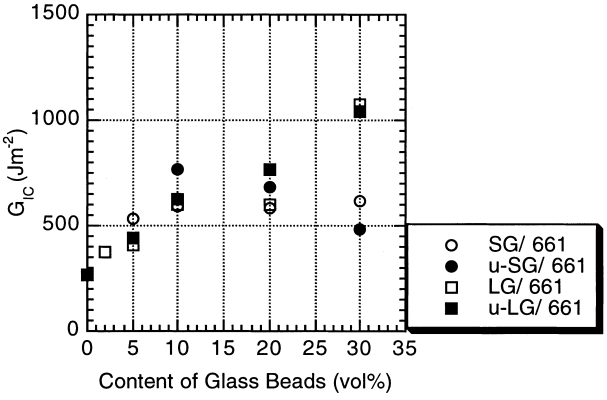

Figure 4 The critical strain energy release rate versus the glass bead content for glass bead filled epoxies.

Furthermore, there may be circumstances under which the effect of thermal residual misfit can screen the effect of surface treatment on the modulus. Even if there are no physical or chemical interactions between the glass beads and matrix, the thermal residual misfit between the glass beads and matrix can produce a certain level of interfacial strength.[23] This is because the coefficient of thermal expansion (CTE) of epoxy is significantly larger than that of glass. A simple estimation[23] gives significant thermal residual misfit stresses, $-\sigma_r = 2\sigma_t \approx 40$ MPa from

$$-\sigma_r = 2\sigma_t = \frac{\Delta\alpha\Delta T}{\left(1 + \frac{\nu_m}{2E_m}\right) + \left(1 - \frac{2\nu_p}{E_p}\right)} \approx \Delta\alpha\Delta T E_m \tag{3}$$

where σ_r is the radial stress, σ_t is the hoop stress, $\Delta\alpha$ is the differential CTE between the matrix and particles ($\alpha_m - \alpha_p$), ΔT is the temperature difference, E is the elastic modulus, ν is Poisson's ratio, and the subscripts m and p indicate the matrix and particles, respectively. [Because of the viscoelastic nature of polymers, the actual values of the thermal residual misfit stresses may be different from those calculated from eq. (3).]

Among various theoretical predictions to determine the moduli of filled composites, one from the equations proposed by Ishai and Cohen[1] is com-

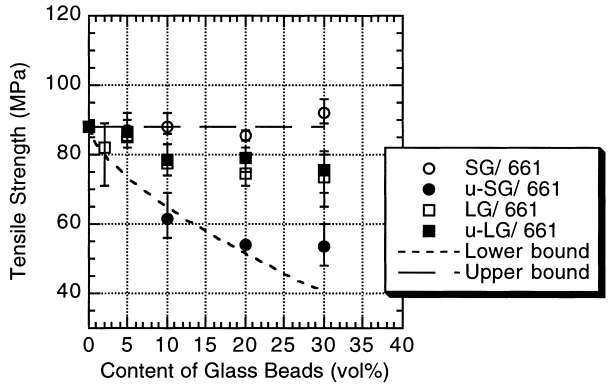

Figure 6 The tensile strength versus the glass bead content for glass bead filled epoxies.

pared with experimental values in Figure 5. The equations are derived from a two-phase model of a cubic matrix containing a cubic inclusion under two conditions: the uniform stress condition

$$\phi_f = \frac{E_c}{E_m} = \frac{1 + (m - 1)C_f^{2/3}}{1 + (m - 1)(C_f^{2/3} - C_f)} \tag{4}$$

and the uniform displacement condition

$$\phi_f = 1 + \frac{C_f}{m/(m - 1) - C_f^{1/3}} \tag{5}$$

where m is E_f/E_m, E_f is the modulus of the fiber, E_m is the modulus of the matrix, E_c is the modulus of the composite, and C_f is the volume fraction of the filler. The theoretical predictions form the upper and lower bounds to the experimental data. Other equations[4,25,26] can also give a similar, reasonable prediction.

The tensile strength (TS) of composites was found to generally decrease as glass bead content increased (Fig. 6). The decrease of the TS was commonly found in inorganic particle toughened systems.[25,27–33] Most data in Figure 6 lie between the two bounds of the simple prediction proposed by Nicolais and Nicodemo.[34] The upper bound is

$$\text{TS} = \sigma_p \tag{6}$$

and the lower bound is

$$\text{TS} = \sigma_p(1 - 1.21C_f^{2/3}) \tag{7}$$

where σ_p is the TS of the polymer and C_f is the volume fraction of inorganic particles. Thus, their simple proposal[34] on the TS of particulate composites seems to be reasonable.

In Figure 6, although the SG/661 systems do not show any significant decrease of tensile strength, the u-SG/661 systems show the largest decrease. The data of the u-SG/661 systems follow the lower bound of the prediction that was derived by treating glass beads as voids. On the other hand, the TS data of the u-LG/661 systems do not show any significant difference from those of the LG/661 systems (Fig. 6).

A possible explanation can be given for the large decrease in the TS of the u-SG/661 systems, which is concerned with the existence of submicron particles on the glass bead surface. It is possible that the number of these particles could be different according to the kinds of glass beads received. Thus, this difference can result in the different TSs of the composites, because these submicron particles can play the role of defects, initiating interfacial failure. Furthermore, submicron particles can induce aggregation of glass beads, because they can easily stay in the interstitial sites and stabilize the aggregates. SG or u-SG systems are more susceptible to aggregation problems than LG or u-LG systems. Apparently, as the size of particles decreases, the aggregates of particles can be more easily stabilized by electrostatic forces and gravitational and mechanical forces that can break aggregates become less important. This explanation is further supported by microscopy studies in a subsequent section.

Figure 6 also shows the effect of glass bead size on tensile strength. This effect can be noticed from the comparison between SG and LG systems, not between u-SG and u-LG systems. This is because the comparison between u-SG and u-LG systems is meaningless when the amounts of submicron particles on the glass bead surface are unknown. In the case of cleaned glass bead systems, the effect of submicron particles can be neglected, because the cleaning process removed most submicron particles (Fig. 2).

Figure 6 obviously reveals that the SG systems have higher tensile strengths than the LG systems. In glass bead filled systems, the critical event leading to tensile failure is most likely the initiation of debonding and growth of cracks. Therefore, the above result is in good agreement with the theories[34–39] for the critical debonding stress (σ_i) or strain (e_i) of inorganic particles in a polymer matrix.

From tensile strength data and the stress distribution functions for infinitely large materials

containing an infinitely sharp crack, the inherent crack size in tensile specimens can be calculated.[6,20,29] The inherent crack size, a, is

$$a = \frac{K_{IC}^2}{\pi(TS)^2} \quad (8)$$

From eq. (8) it is obvious that the inherent crack size will increase as the glass bead content increases, because as it increases the K_{IC} increases and the TS generally decreases, as can be found in Figures 3 and 6. A more interesting result is the change of the inherent crack size according to the size and cleaning process of the glass beads. Because the K_{IC} does not significantly depend on the size and cleaning process of the glass beads (Fig. 3), the differences in the TS will give differences in the inherent crack size: Inherent cracks are smaller in the small glass bead and cleaned systems than in the other systems.

Unfortunately, the calculated values cannot be considered to be the actual inherent crack size existing in tensile specimens. This is because the inherent cracks that initiate the failure of tensile specimens are usually found to be on the surface of specimens, not inside specimens as assumed in the derivation of eq. (8). Furthermore, no real cracks in tensile specimens can be infinitely sharp.

SEM Microscopy Study

The fracture surface of SEN-3PB specimens consists of three different regions,[40,41] i.e., the precrack, process zone, and fast-fracture region. Among them, the process zone is the region where the materials' resistance against crack propagation actually reflects the fracture toughness measured. Both process zone and fast-fracture regions were investigated in this study. More details are available in several references.[9–11]

Figure 7 shows process zones and fast-fracture regions on the fracture surface of 10 vol % SG or u-SG filled epoxies. The wide size distribution of glass beads can be clearly noticed. Crater structures, which are found by the pulling out of glass beads, can be easily found as well. The directions of steps in the process zones show no regular pattern, whereas those in fast-fracture regions are well aligned along the direction of crack propagation. Because all steps result from the formation of separate secondary cracks, the random directions of steps must reflect random local crack propagation directions. The debonding of glass beads can occur ahead of crack tips, particularly while crack fronts are moving stably in the process zone. The resulting isolated secondary cracks have different propagation directions from the primary crack propagation direction. When the primary and the isolated secondary crack fronts meet each other, randomly directed step structures are formed in the process zones. On the other hand, in fast-fracture regions the crack propagation speed is too fast for isolated secondary cracking to occur and grow ahead of the primary crack front. Consequently, only the steps parallel to the primary crack propagation direction result.

In contrast to the fast-fracture regions, the process zones of Figure 7 evidently show debonded glass beads. The existence of debonded glass beads makes debonding zone size measurable using SEM. Debonding zone size is larger in the u-SG system than in the SG system [Fig. 7(A,C)]. This can imply that the interfacial strength between u-SG and the epoxy matrix is lower than that between SG and the matrix. As seen above, the K_{IC} values of both the SG and the u-SG systems are almost the same, regardless of the surface treatments. Thus, the stress and its distributions at break, ahead of crack tips, in both SG and u-SG systems must be similar when the same volume of glass beads is used in both systems.[42] Therefore, if the interfacial strength between the glass beads and matrix is lower, the glass beads farther from a crack tip will debond, resulting in a larger debonding zone size. However, the difference in interfacial strength and debonding zone size could not be correlated with the difference in fracture toughness (Fig. 3). These results actually imply that debonding of glass beads from the matrix may not be the major energy dissipating mechanism for these inorganic particle toughened systems.

Another piece of evidence that shows the different interfacial strengths can be found in the fast-fracture regions of Figure 7(B,D). In these micrographs, more adhesive failure along the interface between the glass beads and matrix is found in the uncleaned system than in the cleaned system. More magnified pictures are provided later, where it is again confirmed that cleaned glass beads have higher interfacial strength than uncleaned glass beads.

Figure 8 shows the fracture surfaces of 10 vol % LG and u-LG filled epoxies. Results similar to those obtained in Figure 7 can be found. First of all, more adhesive failure around the glass beads

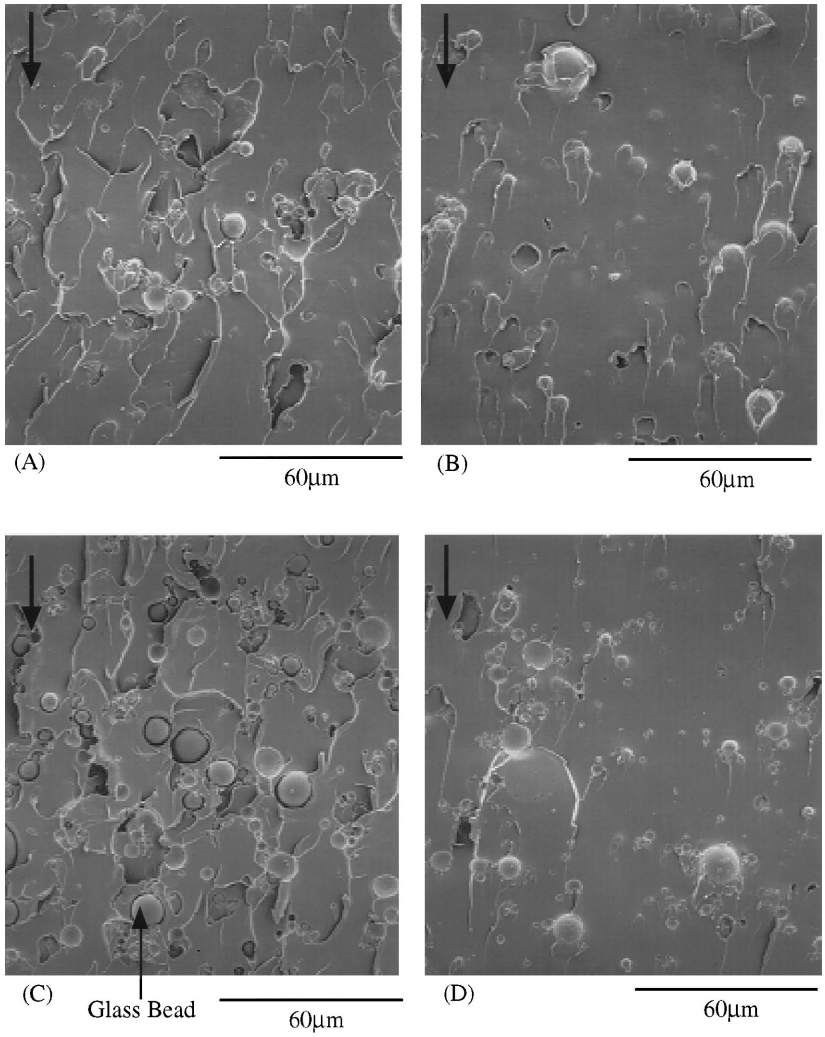

Figure 7 SEM micrographs of the fracture surface of SEN-3PB specimens: (A) the process zone of 10 vol % SG/661, (B) the fast-fracture region of 10 vol % SG/661, (C) the process zone of 10 vol % u-SG/661, and (D) the fast-fracture region of 10 vol % u-SG/661. The arrows indicate the direction of crack propagation.

can be found in the uncleaned system [Fig. 8(D)] than the cleaned system [Fig. 8(B)]. A comparison of the two process zone sizes is rather difficult, because the border of the process zone is obscure. The process zone is confined in a very small area (in the middle of the micrographs) where glass beads are partially or fully debonded [Fig. 8(A)]. In this case, the process zone is almost a line.

The process zone sizes can be more accurately measured by using the three major features of the process zone visible under optical microscopes: debonded glass beads, crack arrest lines, and basic longitudinal textures (BLTs).[43,44] The crack arrest line is formed on the fracture surface when a crack front is arrested for a certain period of time. This is observable in both SEM and OM micrographs because a small amount of tilting exists between the two crack planes behind and ahead of this arrest line. The BLT[43,44] is a fine step structure visible only at high magnification (i.e., higher than about $\times 1000$). It is visible on the fracture surface of all brittle polymers, and its wavelength (periodicity) is approximately 0.2 to 1 μm. Robertson and coworkers[43,44] proposed that liquefaction of the material at the crack tip leads to the formation of this texture. Fortunately, the longitudinal texture is more complicated and the crack arrest line is more visible in the process zone than in the fast-fracture region. These differences make the measurement of the process

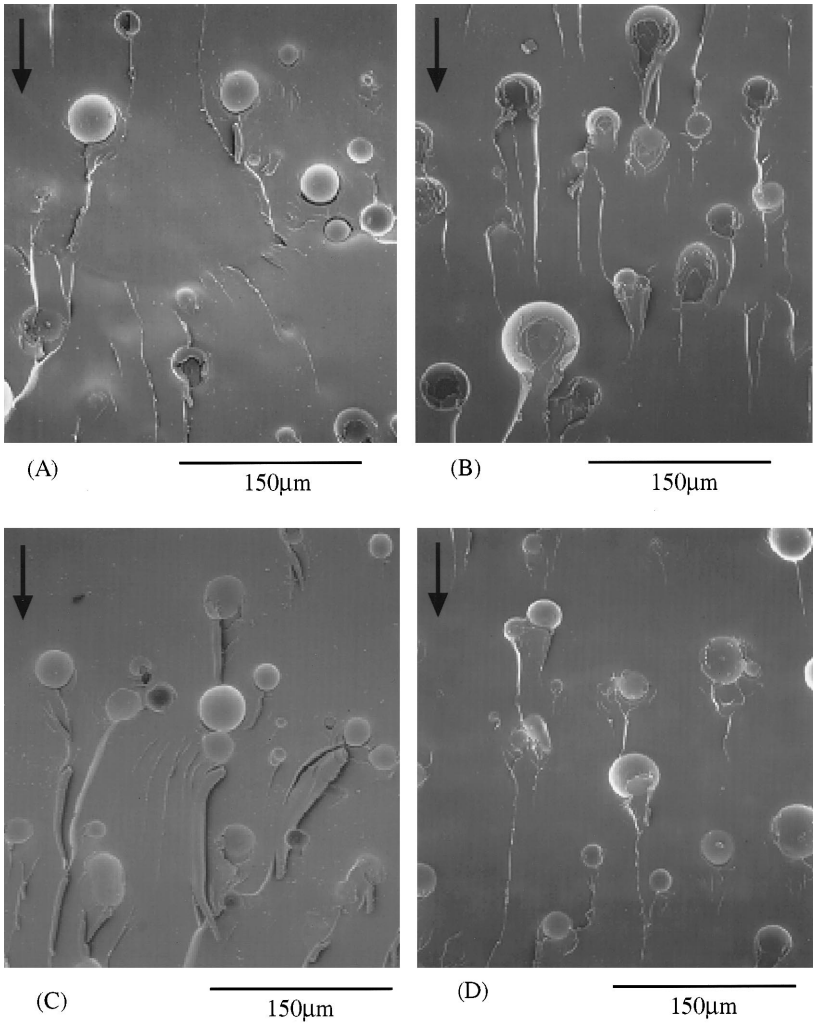

Figure 8 SEM micrographs of the fracture surface of SEN-3PB specimens: (A) the process zone of 10 vol % LG/661, (B) the fast-fracture region of 10 vol % LG/661, (C) the process zone of 10 vol % u-LG/661, and (D) the fast-fracture region of 10 vol % u-LG/661. The arrows indicate the direction of crack propagation.

zone size possible. From these measurements it was found that cleaning the glass beads decreases the process zone size of 10 vol % glass bead content systems (e.g., the average process zone sizes of 10 vol % LG and u-LG systems from 15 measurements were found to be 54 and 125 μm, respectively[9–11]).

Another qualitative assessment of the interfacial strength between glass beads and epoxy matrix can be confirmed by uniaxial tensile tests. During the tests, the tangential modulus of the composites decreases as more glass beads debond from the matrix with loading. If $e_{0.8E}$ is defined as the strain where the tangential modulus drops to 80% of the initial Young's modulus, this value can be treated as a measure of the interfacial strength between the glass beads and matrix. The $e_{0.8E}$ values for 10 vol % LG and u-LG filled epoxies are 1.40 and 1.28%, respectively. These values are still lower than that of unmodified (pure) epoxies (1.60%).

All the results discussed above show that the cleaning process using distilled water can remove submicron particles from the surface of glass beads, thus improving the interfacial strength between the glass beads and the matrix. Figure 9 also illustrates the improved interfacial strength by this process. While u-SG and u-LG systems show more adhesive failure, SG and LG systems show more cohesive failure around the glass beads. This difference in failure mode due to the cleaning process is more pronounced in SG sys-

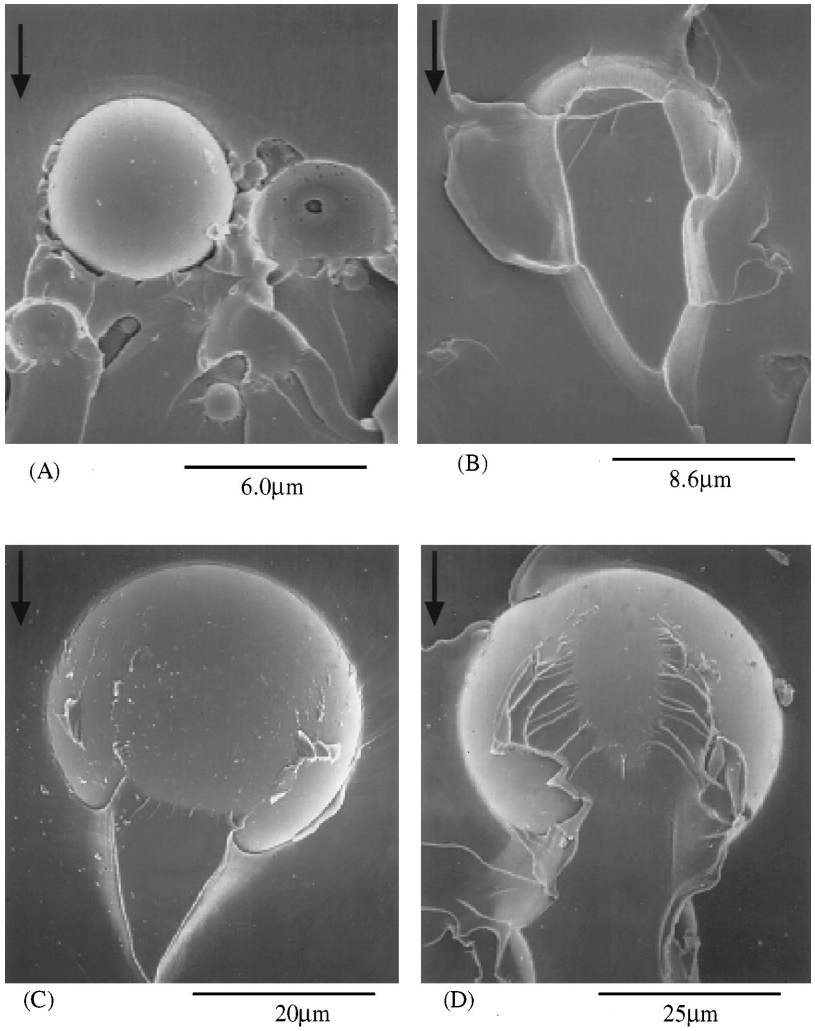

Figure 9 Typical SEM micrographs of glass beads in the fast-fracture region of the fracture surface of SEN-3PB specimens: (A) 10 vol % u-SG/661, (B) 10 vol % SG/661, (C) 10 vol % u-LG/661, and (D) 10 vol % LG/661. The arrows indicate the direction of crack propagation.

tems than in LG systems. This is consistent with the TS data in Figure 6.

If the improvement of interfacial strength by the cleaning process results only from removing submicron particles, then the use of ultrasonic vibration in a different medium must produce the same improvement of interfacial strength. This proposition was found to be true in our experiments. We found that epoxies filled with isopropanol cleaned glass beads (without ultrasonic vibration) showed the same fracture surface features as the u-SG/661 in Figure 7. (Their fracture toughness was also found to be the same as that of u-SG/661 within its experimental error.[9–11]) Therefore, it is true that isopropanol alone cannot improve the interfacial strength. On the other hand, the epoxy in Figure 10 shows the improvement of interfacial strength, which is comparable to that in Figures 7(B) and 9(B). The glass beads in this composite had been cleaned in isopropanol with ultrasonic vibration as described earlier. If a chemical event related to water plays the major role in improving interfacial strength, then the effect of ultrasonic vibration should not be noticed in this composite. Accordingly, this result can support the conclusion that removing submicron particles is the main reason for the improvement of interfacial strength.

Because submicron particles were found in all four kinds of glass beads used in our experiment

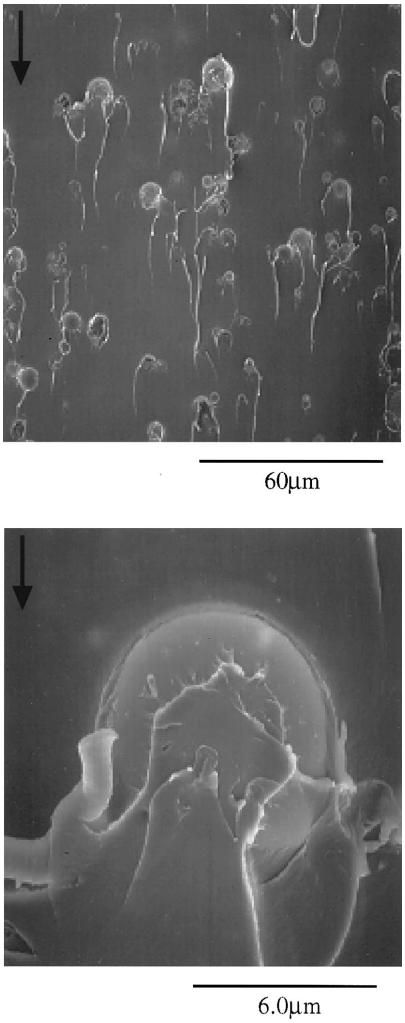

Figure 10 SEM micrographs of the fracture surface (fast-fracture region) of an SEN-3PB specimen composed of epoxy filled with glass beads (10 vol % SG) cleaned with isopropanol in an ultrasonic bath. The arrows indicate the direction of crack propagation.

and may not be effectively removed by some cleaning processes, their existence must be a matter of concern in the preparation of particulate composites. However, the chemical identification of these submicron particles was not attempted in this research. Thus, future research on this subject is needed.

CONCLUSIONS

Epoxies containing glass beads cleaned with distilled water and isopropanol were prepared and their fracture behavior was investigated and compared with that of epoxies containing as-received glass beads. The fracture toughness of the composites was not influenced by the cleaning process, but the interfacial strength between the glass beads and epoxy matrix was. Cleaning glass beads with distilled water was found to remove a significant amount of submicron particles, which existed on the surface of the as-received glass beads. The favorable surface energy of water against the glass beads, not the chemical reactivity, may be the main reason for its removing power. In our experiment, ultrasonic vibration could produce the same removing effect. By removing submicron particles, the cleaning process improved the interfacial strength between the glass beads and matrix and decreased the debonding zone size of 10 vol % glass bead systems. The improvement of interfacial strength can be understood by the fact that the submicron particles on the glass bead surface could behave as defects, initiating interfacial failure.

The authors would like to thank Dr. Hajime Kishi, Dr. Jack Huang, Dr. Cheol Park, and Ms. Jacqueline M. Denoyer for their help.

REFERENCES

1. Ishai, O.; Cohen, L. J. Int J Mech Sci 1967, 9, 539.
2. Ramsteiner, F.; Theysohn, R. Composites 1984, 15, 121.
3. Rothon, R. Particulate-filled Polymer Composites; Longman Scientific & Technical: Essex, U.K., 1995.
4. Nielsen, L. E.; Landel, R. F. Mechanical Properties of Polymers, Composites; Marcel Dekker: New York, 1994; 2nd ed.
5. Marder, M.; Fineberg, J. Phys Today 1996, September, 24.
6. Kinloch, A. J.; Young, R. J. Fracture Behavior of Polymers; Elsevier Applied Science: New York, 1985.
7. (a) Spanoudakis, J.; Young, R. J. J Mater Sci 1984, 19, 473; (b) Spanoudakis, J.; Young, R. J. J Mater Sci 1984, 19, 487.
8. Dekkers, M. E. J.; Dormans, J. P. M.; Heikens, D. Polym Commun 1985, 26, 145.
9. Lee, J. Ph.D. Dissertation, The University of Michigan, 1998.
10. (a) Lee, J.; Yee, A. F. Polymer 2000, 41, 8375; (b) Lee, J.; Yee, A. F. Polymer 2000, 41, 8363; (c) Lee, J.; Yee, A. F. Polymer 2001, 42, 577; (d) Lee, J.; Yee, A. F. Polymer 2001, 42, 589.
11. (a) Lee, J.; Yee, A. F. Polym Prepr Am Chem Soc Div Polym Chem 1997, 38, 369; (b) Lee, J.; Yee, A. F. Polym Prepr Am Chem Soc Div Polym Mater 1998, 79, 200.

12. Brown, W. F.; Srawley, J. E. ASTM STP 381; American Society for Testing and Materials: Philadelphia, 1965; p 13.
13. Hertzberg, R. W. Deformation and Fracture Mechanics of Engineering Materials; Wiley: New York, 1989.
14. Simmons, C. J.; El-Bayoumi, D. H. Experimental Techniques of Glass Science; American Ceramic Society: Westerville, OH, 1993.
15. Morey, G. W. The Properties of Glass; American Chemical Society: New York, 1938.
16. VanKrevelen, D. W.; Hoftyzer, P. J. Properties of Polymers; Elsevier: New York, 1976.
17. Mellan, I. Industrial Solvents Handbook; Noyes Data: Park Ridge, NJ, 1977.
18. Wambach, A.; Trachte, K.; Dibenedetto, A. J Compos Mater 1968, 2, 266.
19. Plueddemann, E. P. Silane Coupling Agent; Plenum: New York, 1982.
20. Moloney, A. C.; Kausch, H. H.; Stieger, H. R. J Mater Sci 1983, 18, 208.
21. Sahu, S.; Broutman, L. J. Polym Eng Sci 1972, 12, 91.
22. Broutman, L. J.; Shau, S. Mater Sci Eng 1971, 8, 98.
23. Clyne, T. W.; Withers, P. J. An Introduction to Metal Matrix Composites; Cambridge University Press: New York, 1993.
24. Selsing, J. J Am Ceram Soc 1961, 44, 419.
25. Ahmed, S.; Jones, F. R. J Mater Sci 1990, 25, 4933.
26. Kerner, E. H. Proc Phys Soc (B) 1956, 69, 808.
27. Nicolais, L.; Narkis, M. Polym Eng Sci 1971, 11, 194.
28. Nicolais, L.; Drioli, E.; Landel, R. F. Polymer 1973, 14, 21.
29. Mallick, P. K.; Broutman, L. J. Mater Sci Eng 1975, 18, 63.
30. Abate, G. F.; Heikens, D. Polym Commun 1983, 24, 342.
31. Smith, J. W.; Kaiser, T.; Roulin-Moloney, A. C. J Mater Sci 1988, 23, 3833.
32. Srivastava, V. K.; Shembekar, P. S. J Mater Sci 1990, 25, 3513.
33. Sjogren, B. A.; Berglund, L. A. Polym Compos 1997, 18, 1.
34. Nicolais, L.; Nicodemo, L. Polym Eng Sci 1973, 13, 460.
35. Gent, A. N. J Mater Sci 1980, 15, 2884.
36. Pukanszky, B.; Van Es, M.; Maurer, F. H. J.; Voros, G. J Mater Sci 1994, 29, 2350.
37. Zhong, X. A.; Knauss, W. G. J Eng Mater Technol 1997, 119, 199.
38. Cho, K.; Gent, A. N. J Mater Sci 1988, 23, 141.
39. Knauss, W. G.; Mueller, H. K. Composite Materials; Sih, G. S., Tamuzs, V. P., Eds.; Sijthoff and Noordhoff, 1979.
40. Yee, A. F.; Pearson, R. A. J Mater Sci 1986, 21, 2462.
41. Pearson, R. A.; Yee, A. F. J Mater Sci 1986, 21, 2475.
42. Williams, J. G. Fracture Mechanics of Polymers; Ellis Horwood Limited, 1984; 1st ed.
43. Covavisaruch, J. S.; Robertson, R. E.; Filisko, F. E. J Mater Sci 1992, 27, 990.
44. Nichols, M. E.; Robertson, R. E. J Mater Sci 1994, 29, 5916.
45. Bucknall, C. B.; Partridge, I. K. Polym Eng Sci 1986, 26, 54.